

Black Hole-Neutron Star Binary Merger Calculations: GRB Progenitors and the Stability of Mass Transfer

Joshua A. Faber^{*,†}, Thomas W. Baumgarte^{**}, Stuart L. Shapiro^{*,‡}, Keisuke Taniguchi^{*} and Frederic A. Rasio[§]

^{*}*Dept. of Physics, University of Illinois at Urbana-Champaign, Urbana, IL 61801, USA*

[†]*NSF Astronomy and Astrophysics Postdoctoral Fellow*

^{**}*Dept. of Physics and Astronomy, Bowdoin College, Brunswick, ME 04011 USA*

[‡]*Dept. of Astronomy and NCSA, UIUC*

[§]*Dept. of Physics and Astronomy, Northwestern University, Evanston, IL 60208 USA*

Abstract. We have calculated the first dynamical evolutions of merging black hole-neutron star binaries that treat the combined spacetime in a nonperturbative general relativistic framework. Using the conformal flatness approximation, we have studied how the location of the tidal disruption radius with respect to the black hole horizon and innermost stable circular orbit (ISCO) affects the qualitative evolution of the system. Based on simple arguments, we show that for a binary mass ratio $q \gtrsim 0.24$, tidal disruption occurs outside the ISCO, while the opposite is true for $q \lesssim 0.24$. When tidal disruption occurs sufficiently far outside the ISCO, mass is transferred unstably from the neutron star to the black hole, resulting in the complete disruption of the neutron star. When tidal disruption occurs slightly within the ISCO, we find that some of the mass forms an extremely hot disk around the black hole. The resulting configurations in this case are excellent candidates for the progenitors of short-hard gamma ray bursts.

Keywords: Black Holes, Neutron Stars, Gamma Ray Bursts, Gravitational Radiation

PACS: 04.30.Db, 04.25.Dm, 47.11.+j, 95.85.Sz

INTRODUCTION

The mergers of compact object binaries consisting of either neutron stars (NSs) or black holes (BHs) are promising sources of gravitational radiation, which hopefully will be detected soon by both ground-based interferometers such as LIGO [1] and the proposed space-based mission LISA [2]. Understanding the evolution of these systems during and after merger, including their emission in gravitational and, for systems containing NSs electromagnetic and neutrino radiation, requires a careful treatment of the relativistic dynamics (see [3] for a recent review). A great deal of effort over the past decade has gone into studying NSNS mergers, and recent treatments incorporate both fully general relativistic gravitation as well as physically realistic nuclear equations of state (EOS) [4, 5]. More recently, there has been a rapid burst of progress on numerical evolution of merging BHBH binaries. Pretorius [6] has performed a stable evolution of the merger of two equal-mass BHs, through the implementation of generalized harmonic coordinates. Several groups have reported comparable results for binary “puncture” BHs, reporting numerical implementations based on the BSSN formulation of Einstein’s equations [7, 8], which seem to be considerably more stable than any previous treatment [9–13].

By contrast, BHNS mergers have received significantly less attention, even though they represent a significant fraction of compact object mergers visible in gravity waves (GWs) [14]. With the exception of the work described herein [15, 16, hereafter papers 1 and 2, respectively], all other calculations of BHNS mergers involve either Newtonian or pseudo-Newtonian gravitational treatments of the NS self-gravity [17], or the entire binary [18–20]. However, as we show here, general relativistic effects play an extremely important role during the tidal disruption of the NS, which occurs in the strong-field regime. This is especially true when the NS disrupts within the ISCO, since the deep relativistic gravitational potential decreases the mass of ejected material while simultaneously increasing the characteristic energy scale associated with it. In order to perform these calculations, we use fully relativistic initial data that solve the conformal thin-sandwich (CTS) equations for quasi-equilibrium BHNS configurations in circular orbits, under the assumption that the BH mass is significantly larger than that of the NS ($q \equiv M_{\text{NS}}/M_{\text{BH}} \ll 1$). These initial data were first derived for synchronized configurations in [21], and then extended to irrotational configurations in [22].

A proper study of BHNS mergers is even more important today in light of the recent localizations of short-hard gamma-ray bursts (SGRBs) for the first time. Long-soft bursts had been previously localized, and several had been seen in coincidence with Type Ib/c supernovae, indicating that they represented the collapse of massive stars [23]. By observing the X-ray afterglow of SGRBs, the *Swift* and *HETE-2* satellites have finally allowed us to identify where SGRBs occur, and in many cases indicate the galaxy that served as host. The rapidly growing list of localized bursts now includes GRBs 050509b, 050724, 050813, and 051221 seen by *Swift*, and GRB 050709 seen by *HETE-2*. Details about each of these, including the physical parameters observed and inferred from these bursts, as well as a complete set of observational references, can be found in Berger [24]. In all cases, the inferred host had a rather low star-formation rate: nearly zero for the putative hosts of 050509b, 050724, and 050813, while significantly higher but still low relative to long GRB hosts for 050709 and 051221 [25, 26]. Massive stars have very short lifetimes and are typically found in regions with high star formation, so these observations favor the identification of a compact object binary merger as the progenitor, as originally suggested by Paczynski [27]. A significant fraction of both neutron star-neutron star (NSNS) and black hole-neutron star (BHNS) binaries, on the other hand, will take longer than 1 Gyr between formation and merger [28].

While our work here has focused on BHNS mergers, we note that fully general relativistic calculations of NSNS mergers suggest that they are also strong candidates for producing SGRBs. The standard schematic model for merger-induced short-duration GRBs involves creating a hot, massive ($M > 0.01M_{\odot}$) accretion disk around a spinning BH (see Piran [29] for a thorough review). Recent fully general relativistic calculations show that such configurations naturally result from either of two distinct formation channels in NSNS mergers. For NSs of significantly different masses (mass ratios $q \lesssim 0.7$), tidal disruption of the lighter NS produces a heavy disk that will accrete onto a newly formed BH at the binary center-of-mass [4, 5]. Alternately, for more equal-mass systems, the merger may produce a hypermassive neutron star (HMNS), supported against gravitational collapse by differential rotation with a total mass heavier than the maximum allowed mass for uniformly rotating configurations [30, 31]. Magnetohydrodynamic (MHD) simulations in full GR show that the HMNS undergoes a delayed collapse, resulting in a hot, magnetized torus surrounding a rotating BH, together with a magnetic field collimated along the polar axis. These conditions are favorable for a burst powered either by neutrino annihilation or MHD effects [32, 33].

As we discuss at length in Paper 2, it is very difficult to determine whether current observations favor the likely progenitors of SGRBs to be NSNS mergers, BHNS mergers, or possibly both. While the most recent calculations of the SGRB merger rate, $\mathcal{R}_{GRB} \sim 1 - 3 \text{ Myr}^{-1}$ per Milky Way Galaxy [34, 35] seem to be higher than previously estimated, the predicted merger rates from population synthesis calculations and other methods are still uncertain by up to two orders of magnitude [28, 36, 37]. Moreover, the projected distance from a localized SGRB to the center of its host galaxy is insensitive to whether the merging binary is an NSNS or BHNS system, since the projected distance likelihood functions for both BHNS and NSNS mergers are very close for a wide range of galaxy masses [38].

Perhaps the strongest constraint on possible GRB progenitors involves the density of baryons around the central engine along the polar axes. The low energy measured for GRB 050509b, $E_{\gamma} = 3 \times 10^{48}$ erg, argues for an extremely low density of baryons surrounding the GRB, assuming that it occurred at the inferred redshift $z = 0.225$ and the Lorentz factor of the jet Γ is no bigger than the ratio η of the energy in the jet to the rest energy of the baryons through which it must travel, $\Gamma \leq \eta \equiv E_{\gamma}/M_b c^2$ [39]. For a typical Lorentz factor $\Gamma \gtrsim 100$ [40], at most $10^{-8}(\Omega/4\pi)M_{\odot}$ of material can surround the progenitor, where Ω is the solid angle of the GRB jet.

NUMERICAL TECHNIQUES

We performed dynamical 3+1-dimensional smoothed particle hydrodynamics (SPH) calculations of BHNS mergers in the conformal flatness (CF) approximation of GR [41, 42]. For test masses in orbit about Schwarzschild BHs our scheme identifies the relativistic ISCO exactly and accounts for relativistic dynamics within the ISCO, unlike previous pseudo-Newtonian calculations [18–20]. Quasi-equilibrium initial data can also be constructed to be conformally flat, so that they are consistent with our evolution scheme. During the dynamical evolution the CF assumption is only approximate, since in general the spatial metric would not remain conformally flat, but we expect these deviations to be small. Our calculations of BHNS coalescence make use of a simplifying technique introduced by Baumgarte et al. [21]: by assuming an extreme mass ratio ($q \ll 1$), we may hold the BH position fixed in space and solve the field equations for the combined spacetime in a domain surrounding the NS but outside the BH. The resulting solution represents the fully dynamical field configuration under our assumptions.

Our numerical scheme is discussed in detail in Papers 1 and 2. There, we evolved the matter adiabatically, but accounting for shocks, by solving the coupled nonlinear elliptic field equations with either the Lorene spectral

methods libraries, publicly available at <http://www.lorene.obspm.fr>, or via iterated FFT convolution. We include artificial viscosity effects through a relativistic generalization of the form found in [43].

The defining parameter for determining the qualitative evolution of a BHNS merger is the binary mass ratio $q \equiv M_{\text{NS}}/M_{\text{BH}}$. Assuming that the tidal disruption of the NS begins at a separation a_{R} where its volume in isolation is equal to the volume of its Roche lobe,

$$a_{\text{R}}/M_{\text{BH}} = 2.17q^{2/3}(1+q)^{1/3}\mathcal{C}^{-1} \quad (1)$$

for a NS of compactness $\mathcal{C} \equiv M_{\text{NS}}/R_{\text{NS}}$ [44], using geometrized units with $G = c = 1$.

Much of the previous discussion of BHNS mergers has portrayed the outcome of these events as a simple process following one of two evolutionary paths. If disruption occurs outside the innermost stable circular orbit (ISCO), the NS transfers mass onto the BH. This widens the orbit, leading to either a long-term stable mass transfer phase [45, 46], or punctuated phases of Roche lobe overflow [47]. For a sufficiently large BH (and thus small q), a_{R} is smaller than the innermost stable circular orbit (ISCO), a_{ISCO} , so that the NS passes through the ISCO before being tidally disrupted. For a typical NS of compactness $\mathcal{C} = 0.15$ the critical mass ratio at which tidal disruption occurs at a_{ISCO} is approximately $q_{\text{crit}} = 0.24$. For binaries with $q < q_{\text{crit}}$, it has typically been suggested that the NS will be swallowed whole by the BH [48]. As we show below, these simple assumptions about dynamics fail to describe the complicated processes seen in numerical calculations.

We cannot directly simulate the physical realistic “critical case” ($q = q_c = 0.24$, $\mathcal{C} = 0.15$) that disrupts at the ISCO, nor those with lower-mass BHs in which the NS disrupts outside the ISCO, since they violate our assumption of an extreme mass ratio. We can, however, evolve configurations with arbitrary values of a_{R} by instead altering the NS compactness while holding the mass ratio fixed at $q = 0.1$. In Paper 1, we studied the case where the NS disrupts outside the ISCO by studying the evolution of a NS with compactness $M/R = 0.042$ in a binary of mass ratio $q = 0.1$. The NS was taken to be initially corotating. We consider first the results from run B3a of Paper 1, which featured a NS with a polytropic EOS with adiabatic index $\Gamma = 2$. To study disruption within the ISCO we calculated the evolution of binaries with the same mass ratio and NS EOS, but compactness 0.14 and 0.09 (runs 1 and 2, respectively of Paper 2). The latter of these is expected to disrupt at a binary separation $a_{\text{R}} = 5.3M_{\text{BH}}$, just within the ISCO, and serves as our model for the critical case. For these two runs, the initial configuration is irrotational, which is expected to be the physically realistic case.

DISRUPTION OUTSIDE THE ISCO: UNSTABLE MASS TRANSFER

For NS disruption outside the ISCO, the relevant timescales rule out initially stable mass transfer. When mass transfer begins, the NS has a significant infall velocity, and it requires a significant fraction of an orbit to reverse this velocity and allow the NS to spiral outward. During this time, mass loss through the inner Lagrange point accelerates, stripping a great deal of matter from the NS. Unless the actual NS EOS is extremely stiff, mass transfer will not stabilize, and the NS will be completely disrupted. We illustrate of this process in Figs. 1 and 2.

We see that mass transfer begins slowly, funneling matter through the inner Lagrange point directly onto the BH. During the first orbit after this, the mass transfer rate increases, since the Lagrange point actually moves inward into the outer layers of the NS. Eventually, the NS expands in response to mass loss, and matter is lost through the outer Lagrange point as well. The effect of the NS is catastrophic: matter lost outward yields a net inward force that slows the widening of the orbit, preventing mass transfer from stabilizing. As a result, the NS spirals outward at a rate too slow to quench the mass loss, and is completely disrupted within another orbit.

We expect the evolution of the binary to follow this qualitative path for BHs not much more massive than the NS ($q \gtrsim 0.3$), even if the NS EOS is very stiff. If mass loss can actually be quenched, it will occur while the NS moves outward on an elliptical orbit. Unlike the model presented in [47], however, we expect that mass transfer will begin again during the next approach toward pericenter, since there is no obvious means to provide the angular momentum kick that their model presupposes to boost the NS into a wider orbit.

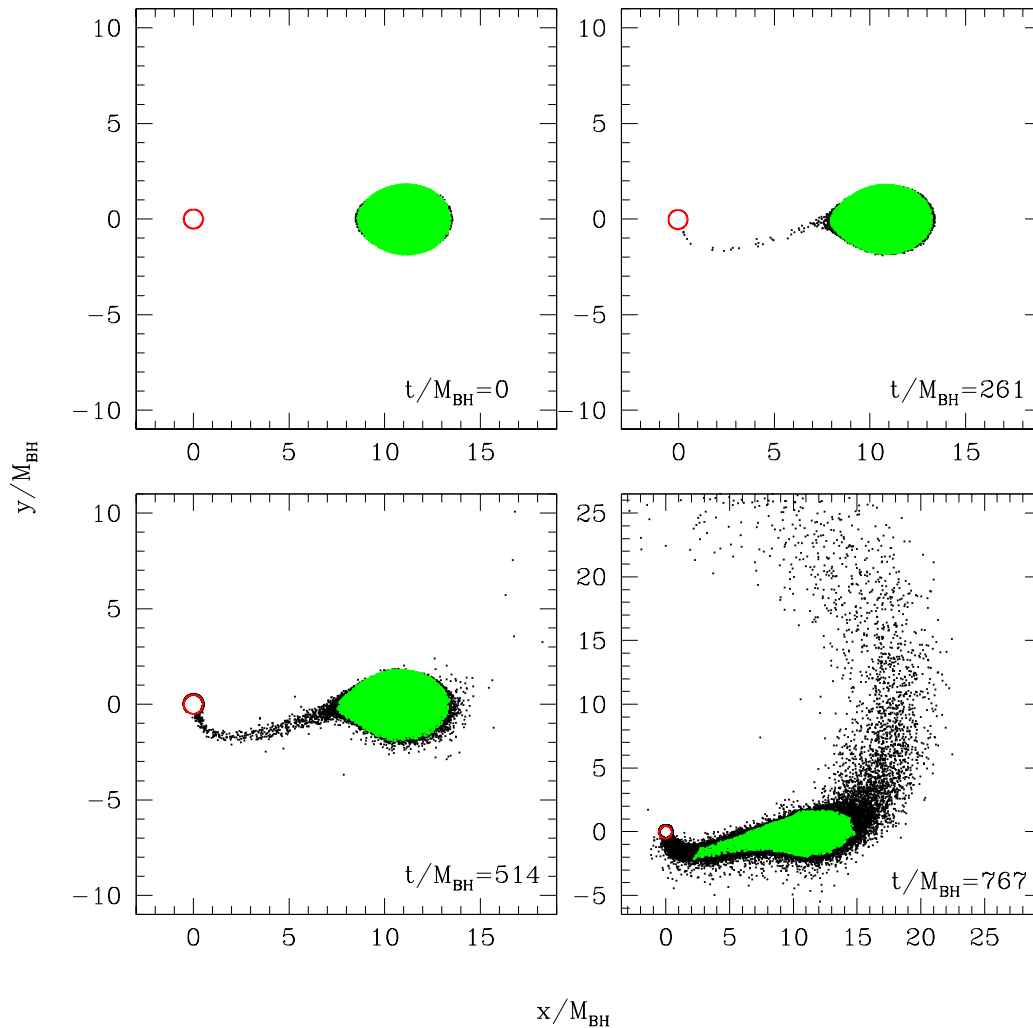


FIGURE 1. Snapshots of the fluid configuration projected into the orbital plane initially, and after 1, 2, and 3 full orbits. The NS has a compactness $M/R = 0.042$ and the binary mass ratio is $M_{\text{NS}}/M_{\text{BH}} = 0.1$. Mass lost through the inner Lagrange point accretes directly onto the BH for an orbit, at an increasing rate. When the NS begins to expand, mass is lost through both the inner and outer Lagrange points, leading to the complete disruption of the NS.

DISRUPTION INSIDE THE ISCO: DISK FORMATION AND IMPLICATIONS FOR SGRBS

To study disruption within the ISCO, we consider two models, both containing $n = 1$ polytropes. First is a NS of compactness 0.14 in a binary of mass ratio $q = 0.1$, for which $a_{\text{R}} = 3.2M_{\text{BH}}$ according to Eq. 1. For this case, referred to as run 1 in Paper 2, the NS is accreted completely by the BH, as tidal disruption begins once the NS has already begun to approach the horizon. Essentially no matter is ejected. Such a model is unlikely to produce a large luminosity in neutrinos, as the matter never shocks as it falls onto the BH. The GW signal from such an event may be significant, both from the prior inspiral and the subsequent BH ringing, but determining the exact GW signal requires a fully non-conformally flat, general relativistic treatment that is beyond the capabilities of our current code.

The more exciting case for producing an electromagnetic signal is run 2 of Paper 2, a NS of compactness 0.09 in a binary of mass ratio $q = 0.1$, which disrupts just inside the ISCO, as shown in Fig. 3. Note that radii in the figure are measured in isotropic coordinates. When tidal disruption begins after nearly two orbits, as seen in the second panel, 98% of the NS mass lies within the ISCO. From this point onward, however, rapid redistribution of angular momentum

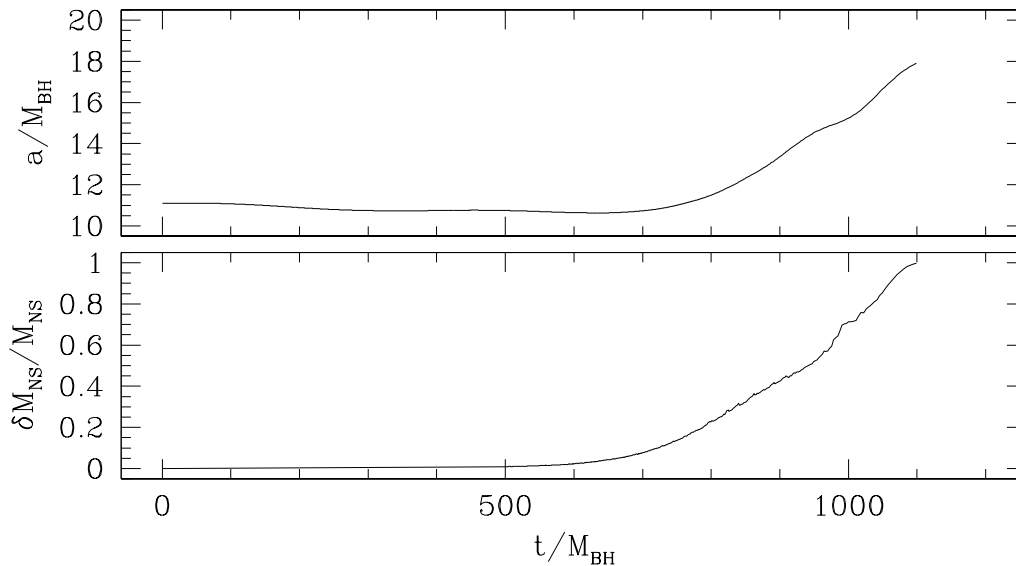


FIGURE 2. Binary separation a/M_{BH} (top) and fractional mass $\delta M/M_{\text{NS}}$ lost from the NS (bottom) as a function of time, for the run shown in Fig. 1. We see that mass loss is accompanied by a gradual increase in the orbital separation, but continues unquenched until the NS is completely disrupted.

allows a great deal more mass, $\sim 0.25M_{\text{NS}}$, to be expelled outside the ISCO, while the remaining fraction, $0.75M_{\text{NS}}$, is accreted promptly by the BH.

While half of the ejected matter is unbound from the system, the remaining fraction, $\sim 0.12M_{\text{NS}}$, will eventually fall back and form a disk located just outside the ISCO. This configuration satisfies all the geometric constraints required for a GRB progenitor, as all matter lies in the equatorial plane rather than the polar axis. The bound matter in the disk is relatively cold at first, as the matter in the arm is initially ejected without strong shock heating. Over time, this disk generates heat via shocks and expands vertically into a torus out to a radius of $r \sim 50M_{\text{BH}}$ within $t = 1000M_{\text{BH}} \sim 0.07$ s; (see Fig. 4).

The specific internal energy in the inner part of the torus corresponds to a temperature $T \approx 3 - 10 \text{ MeV} \approx 2 - 7 \times 10^{10} \text{ K}$, shown in Fig. 5. The surface density in this region is $\Sigma \approx 2 - 3 \times 10^{17} \text{ g cm}^{-2}$. Assuming an opacity $\kappa = 7 \times 10^{-17} (T/10^{11} \text{ K})^2$, we conclude that the disk is optically thick out to $r \sim 15M$. In the diffusion limit, the neutrino flux is $F_{\nu} \approx 7\sigma T^4 / \kappa \Sigma$ where σ is the Stefan-Boltzmann constant. The total neutrino luminosity is $L_{\nu} \approx 2\pi r^2 F_{\nu} \sim 10^{54} \text{ erg s}^{-1}$, which should be sufficient to generate the annihilation luminosity required to power a SGRB.

Qualitatively, the hot torus described here is similar to that found from collapsing HMNS remnants in NSNS mergers [33], but is physically larger. While we do not follow the long-term evolution of the accretion torus and surrounding material, we can estimate the fallback time for the bound component, assuming geodesic orbits. Approximately $0.03M_{\text{NS}}$ should return back toward the BH on timescales equal to or longer than a second, which could in principle produce lower-energy bursts at later times. It is conceivable that this fallback accretion might explain the secondary X-ray flares observed in SGRBs many seconds after the initial burst (see [24] for a summary of the observations), especially if self-gravity leads to the formation of higher density clumps of material, but further simulations are required to establish this identification.

CONCLUSIONS

Future observations should help to determine which progenitor candidates are responsible for the observed short GRB population. Gravitational wave measurements would provide important evidence if detected in coincidence: A GRB resulting from hypermassive collapse would occur noticeably delayed relative to the gravitational wave signal from

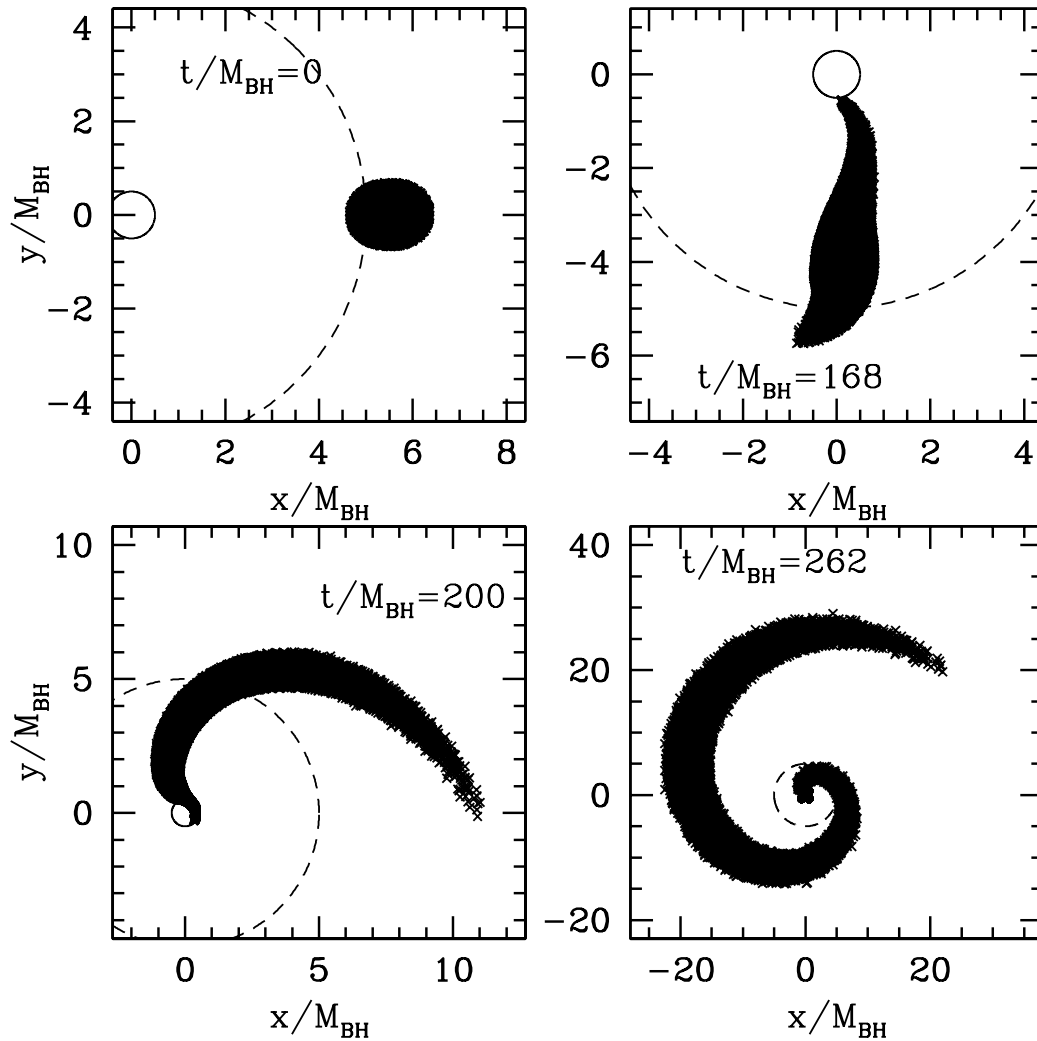


FIGURE 3. Snapshots of configurations taken from run 2 of Paper 2 [16], with conventions as in Fig. 1. The NS has a compactness $M/R = 0.09$ and the binary mass ratio is $M_{\text{NS}}/M_{\text{BH}} = 0.1$. We see the NS disrupts just within the ISCO (dashed curve), producing a mass-transfer stream outward, which eventually wraps around the BH (whose horizon is shown as the solid curve) to form a torus. The initial orbital period is $P = 105M_{\text{BH}}$.

the inspiral and plunge phases of nearly equal-mass objects, whereas one resulting from a BHNS binary would occur almost immediately after the signal from a very unequal-mass merger.

To be able to predict which BHNS binaries would be SGRB progenitor candidates, we need to determine the critical separation for tidal disruption separating cases where the NS is swallowed whole from those where a disk can form, which we have constrained to fall in the range $3M_{\text{BH}} < a_{R;\text{crit}} < 6M_{\text{BH}}$. Of course, a proper study will require us to drop the extreme mass ratio assumption and allow the BH to propagate through the grid. It is unclear that a very sharp transition exists between cases where the NS disrupts just within or just outside the ISCO, since both cases predict that the majority of the NS mass accretes onto the BH while some is ejected outward. We are currently gearing up to study this process in fully general relativistic simulations, relaxing both the assumptions of conformal flatness and extreme mass ratios..

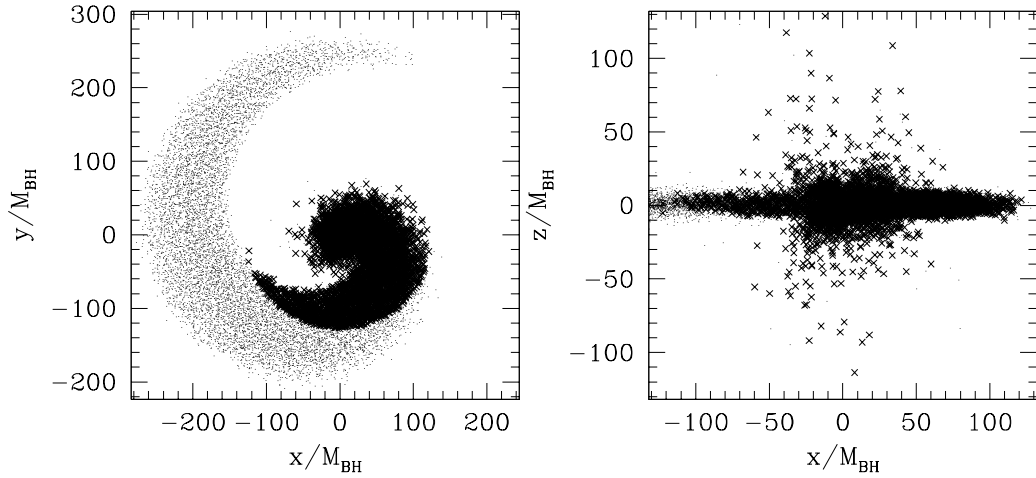


FIGURE 4. Matter configuration at the end of the simulation, $T = 990M_{\text{BH}}$, projected onto the equatorial (left panel) and meridional (right panel) showing the hot torus located within $r < 50M_{\text{BH}}$. Bound fluid elements (satisfying $u_0 - 1 < 0$) are shown as crosses, unbound elements as points. Note the different scales.

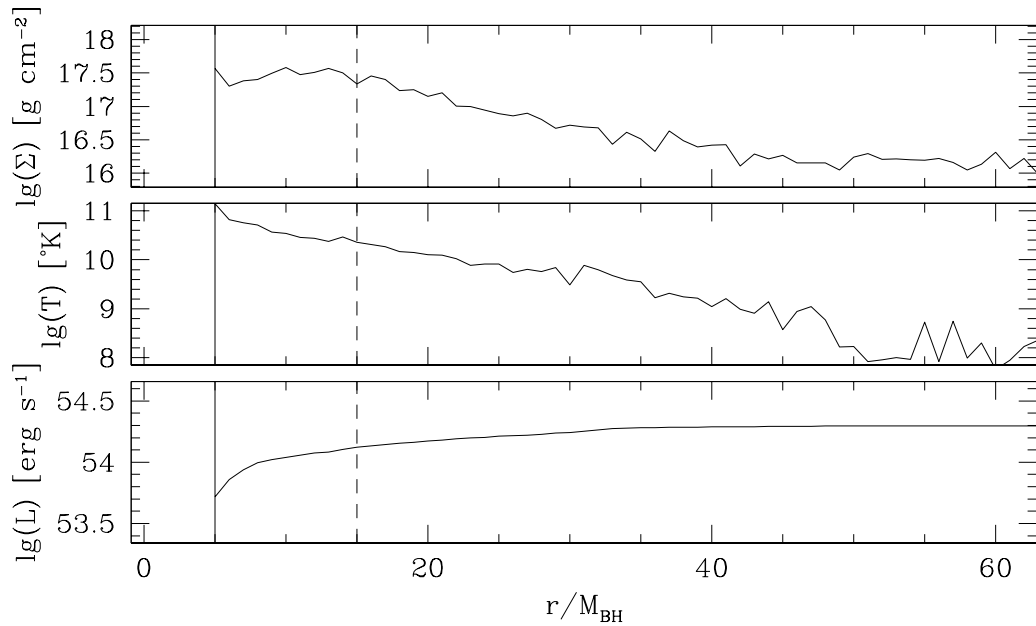


FIGURE 5. Surface density Σ , temperature T , and integrated neutrino luminosity L , as a function of cylindrical radius for the configuration shown in Fig. 4. The solid vertical line denotes the ISCO, and the dashed line the transition radius between matter optically thick to neutrinos within and optically thin outside.

ACKNOWLEDGMENTS

J. A. F. is supported by an NSF Astronomy and Astrophysics Postdoctoral Fellowship under award AST-0401533. T. W. B. gratefully acknowledges support from the J. S. Guggenheim Memorial Foundation. This work was supported

in part by NSF grants PHY-0205155 and PHY-0345151 and NASA Grant NNG04GK54G to the University of Illinois, NSF Grant PHY-0456917 to Bowdoin College, and PHY-0245028 to Northwestern University.

REFERENCES

1. The LIGO Science Collaboration, *Phys. Rev. D* **72**, 082001 (2005), see also <http://www.ligo.org>.
2. K. Danzmann, and the LISA study team, *Classical and Quantum Gravity* **13**, A247–A250 (1996).
3. T. W. Baumgarte, and S. L. Shapiro, *Phys. Rept.* **376**, 41–131 (2003).
4. M. Shibata, K. Taniguchi, and K. Uryū, *Phys. Rev. D* **71**, 084021 (2005).
5. M. Shibata, and K. Taniguchi, *Phys. Rev. D* **73**, 064027 (2006).
6. F. Pretorius, *Phys. Rev. Lett.* **95**, 121101 (2005).
7. M. Shibata, and T. Nakamura, *Phys. Rev. D* **52**, 5428–5444 (1995).
8. T. W. Baumgarte, and S. L. Shapiro, *Phys. Rev. D* **59**, 024007 (1999).
9. J. G. Baker, J. Centrella, D.-I. Choi, M. Koppitz, and J. van Meter, *Phys. Rev. D*, submitted, **gr-qc/0602026** (2006).
10. J. G. Baker, J. Centrella, D.-I. Choi, M. Koppitz, J. R. van Meter, and M. C. Miller, *Astrophys. J. Lett.*, submitted, **astro-ph/0603204** (2006).
11. M. Campanelli, C. O. Lousto, P. Marronetti, and Y. Zlochower, *preprint*, **gr-qc/0511048** (2005).
12. M. Campanelli, C. O. Lousto, and Y. Zlochower, *Phys. Rev. D* **73**, 061501 (2006).
13. F. Herrmann, D. Shoemaker, and P. Laguna, *preprint*, **gr-qc/0601026** (2006).
14. K. Belczynski, V. Kalogera, and T. Bulik, *Astrophys. J.* **572**, 407–431 (2002).
15. J. A. Faber, T. W. Baumgarte, S. L. Shapiro, K. Taniguchi, and F. A. Rasio, *Phys. Rev. D* **73**, 024012 (2006), [Paper 1].
16. J. A. Faber, T. W. Baumgarte, S. L. Shapiro, and K. Taniguchi, *Astrophys. J. Lett.*, accepted, **astro-ph/0603277** (2006), [Paper 2].
17. F. Rasio, J. Faber, S. Kobayashi, and P. Laguna, “Relativistic SPH Calculations of Compact Binary Mergers,” in *Proceedings of JGRG14*, edited by W. Hikida, M. Sasaki, T. Tanaka, and T. Nakamura, 2005, **astro-ph/0503007**.
18. H.-T. Janka, T. Eberl, M. Ruffert, and C. L. Fryer, *Astrophys. J. Lett.* **527**, L39–L42 (1999).
19. W. H. Lee, and W. Ł. Kluźniak, *Astrophys. J.* **526**, 178–199 (1999).
20. S. Rosswog, *preprint*, **astro-ph/0505007** (2005).
21. T. W. Baumgarte, M. L. Skoge, and S. L. Shapiro, *Phys. Rev. D* **70**, 064040 (2004).
22. K. Taniguchi, T. W. Baumgarte, J. A. Faber, and S. L. Shapiro, *Phys. Rev. D* **72**, 044008 (2005).
23. B. Paczynski, *Astrophys. J. Lett.* **494**, L45–L48 (1998).
24. E. Berger, “The Afterglows and Host Galaxies of Short GRBs: An Overview,” in *Gamma Ray Bursts in the Swift Era*, edited by S. Holt, N. Gehrels, and J. Nousek, 2006, **astro-ph/0602004**.
25. J. Hjorth, D. Watson, J. P. U. Fynbo, P. A. Price, B. L. Jensen, U. G. Jørgensen, D. Kubas, J. Gorosabel, P. Jakobsson, J. Sollerman, K. Pedersen, and C. Kouveliotou, *Nature* **437**, 859–861 (2005).
26. A. M. Soderberg, E. Berger, M. Kasliwal, D. A. Frail, P. A. Price, B. P. Schmidt, S. R. Kulkarni, D. B. Fox, S. B. Cenko, K. C. Roth, and A. Gal-Yam, *Astrophys. J.*, submitted, **astro-ph/0601455** (2006).
27. B. Paczynski, *Astrophys. J. Lett.* **308**, L43–L46 (1986).
28. K. Belczynski, T. Bulik, and B. Rudak, *Astrophys. J.* **571**, 394–412 (2002).
29. T. Piran, *Rev. Mod. Phys.* **76**, 1143–1210 (2005).
30. T. W. Baumgarte, S. L. Shapiro, and M. Shibata, *Astrophys. J. Lett.* **528**, L29–L32 (2000).
31. S. L. Shapiro, *Astrophys. J.* **544**, 397–408 (2000).
32. M. D. Duez, Y. T. Liu, S. L. Shapiro, M. Shibata, and B. C. Stephens, *Phys. Rev. Lett.* **96**, 031101 (2006).
33. M. Shibata, M. D. Duez, Y. T. Liu, S. L. Shapiro, and B. C. Stephens, *Phys. Rev. Lett.* **96**, 031102 (2006).
34. D. Guetta, and T. Piran, *preprint*, **astro-ph/0511239** (2005).
35. E. Nakar, A. Gal-Yam, and D. B. Fox, *preprint*, **astro-ph/0511254** (2005).
36. R. Voss, and T. M. Tauris, *Mon. Not. R. Astron. Soc.* **342**, 1169–1184 (2003).
37. V. Kalogera, C. Kim, D. R. Lorimer, M. Burgay, N. D’Amico, A. Possenti, R. N. Manchester, A. G. Lyne, B. C. Joshi, M. A. McLaughlin, M. Kramer, J. M. Sarkissian, and F. Camilo, *Astrophys. J. Lett.* **601**, L179–L182 (2004).
38. K. Belczynski, R. Perna, T. Bulik, V. Kalogera, N. Ivanova, and D. Q. Lamb, *Astrophys. J.*, submitted, **astro-ph/0601458** (2006).
39. A. Shemi, and T. Piran, *Astrophys. J. Lett.* **365**, L55–L58 (1990).
40. R. Oechslin, and H. T. Janka, *Mon. Not. R. Astron. Soc.*, accepted, **astro-ph/0507099** (2005).
41. J. A. Isenberg, *preprint*, *University of Maryland*, unpublished (1978).
42. J. R. Wilson, G. J. Mathews, and P. Marronetti, *Phys. Rev. D* **54**, 1317–1331 (1996).
43. L. Hernquist, and N. Katz, *Astrophys. J. Suppl.* **70**, 419–446 (1989).
44. B. Paczyński, *Ann. Rev. Astron. Astrophys.* **9**, 183 (1971).
45. J. P. A. Clark, and D. M. Eardley, *Astrophys. J.* **215**, 311–322 (1977).
46. S. F. Portegies Zwart, *Astrophys. J. Lett.* **503**, L53–L56 (1998).
47. M. B. Davies, A. J. Levan, and A. R. King, *Mon. Not. R. Astron. Soc.* **356**, 54–58 (2005).
48. M. C. Miller, *Astrophys. J. Lett.* **626**, L41–L44 (2005).